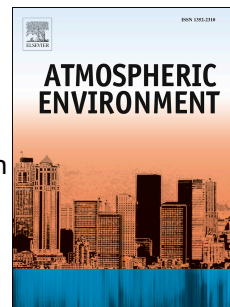


Accepted Manuscript

Linking improvements in sulfur dioxide emissions to decreasing sulfate wet deposition by combining satellite and surface observations with trajectory analysis

Nikita Fedkin, Can Li, Russell R. Dickerson, Timothy Canty, Nickolay A. Krotkov



PII: S1352-2310(18)30819-7

DOI: <https://doi.org/10.1016/j.atmosenv.2018.11.039>

Reference: AEA 16404

To appear in: *Atmospheric Environment*

Received Date: 5 June 2018

Revised Date: 14 November 2018

Accepted Date: 16 November 2018

Please cite this article as: Fedkin, N., Li, C., Dickerson, R.R., Canty, T., Krotkov, N.A., Linking improvements in sulfur dioxide emissions to decreasing sulfate wet deposition by combining satellite and surface observations with trajectory analysis, *Atmospheric Environment* (2018), doi: <https://doi.org/10.1016/j.atmosenv.2018.11.039>.

This is a PDF file of an unedited manuscript that has been accepted for publication. As a service to our customers we are providing this early version of the manuscript. The manuscript will undergo copyediting, typesetting, and review of the resulting proof before it is published in its final form. Please note that during the production process errors may be discovered which could affect the content, and all legal disclaimers that apply to the journal pertain.

1 **Linking Improvements in Sulfur Dioxide Emissions to Decreasing Sulfate Wet Deposition**
2 **by Combining Satellite and Surface Observations with Trajectory Analysis**

3 **Nikita Fedkin¹, Can Li^{2,3}, Russell R. Dickerson¹, Timothy Canty¹, Nickolay A. Krotkov³**
4

5 1: Department of Atmospheric and Oceanic Science, University of Maryland, College Park,
6 Maryland, USA

7 2: Earth System Science Interdisciplinary Center, University of Maryland, College Park,
8 Maryland, USA

9 3: Atmospheric Chemistry and Dynamics Laboratory, NASA Goddard Space Flight Center,
10 Greenbelt,
11

12
13 **Abstract:**

14 Sulfur dioxide (SO₂), a criteria pollutant, and sulfate (SO₄²⁻) deposition are major environmental
15 concerns in the eastern U.S. and both have been on the decline for two decades. In this study, we
16 use satellite column SO₂ data from the Ozone Monitoring Instrument (OMI), and SO₄²⁻ wet
17 deposition data from the NADP (National Atmospheric Deposition Program) to investigate the
18 temporal and spatial relationship between trends in SO₂ emissions and the downward sulfate wet
19 deposition over the eastern U.S. from 2005 to 2015. To establish the relationship between SO₂
20 emission sources and receptor sites, we conducted a Potential Source Contribution Function
21 (PSCF) analysis using HYSPLIT back trajectories for five selected Air Quality System (AQS)
22 sites - (Hackney, OH, Akron, OH, South Fayette, PA, Wilmington, DE, and Beltsville, MD) - in
23 close proximity to NADP sites with large downward SO₄²⁻ trends since 2005. Back trajectories
24 were run for three summers (JJA) and three winters (DJF) and used to generate seasonal
25 climatology PSCFs for each site. The OMI SO₂ and interpolated NADP sulfate deposition trends
26 were normalized and overlapped with the PSCF, to identify the areas that had the highest
27 contribution to the observed drop. The results suggest that emission reductions along the Ohio

28 River Valley have led to decreases in sulfate deposition in eastern OH and western PA (Hackney,
29 Akron and South Fayette). Farther to the east, emission reductions in southeast PA resulted in
30 improvements in sulfate deposition at Wilmington, DE, while for Beltsville, reductions in both
31 the Ohio River Valley and nearby favorably impacted sulfate deposition. For Beltsville, sources
32 closer than 300 km from the site contribute roughly 56% observed deposition trends in winter,
33 and 82% in summer, reflecting seasonal changes in transport pattern as well as faster oxidation
34 and washout of sulfur in summer. This suggests that emissions and wet deposition are linked
35 through not only the location of sources relative to the observing sites, but also to
36 photochemistry and the weather patterns characteristic to the region, as evidenced by a west to
37 east shift in the contribution between winter and summer. The method developed here is
38 applicable to other regions with significant trends such as China and India, and can be used to
39 estimate the potential benefits of emission reduction in those areas.

40

41 **1 Introduction:**

42 Sulfur dioxide (SO_2) and sulfate (SO_4^{2-}) are major pollutants resulting from coal burning
43 and industrial processes. Sulfate wet deposition negatively affects surface and ground water and
44 certain ecosystems through changing chemical characteristics of soil (U.S. EPA, 2003; Butler et
45 al., 2001; Likens et al., 2002). While posing a major pollution problem in the second half of the
46 20th century, both species have shown a definite downward trend in the eastern United States.
47 The reason for their decreases is undisputed – initiatives such as the various phases of the Clean
48 Air Act (U.S. EPA, 2015; Butler et al, 2001) and increased monitoring of pollutants and
49 deposition by EPA’s Acid Rain Program (U.S. EPA, 2002) have led to drastic reductions in
50 sulfur emissions and the subsequent SO_4^{2-} formation, especially in regional hotspots such as the
51 Ohio River Valley. Sulfate is produced chemically in the atmosphere mainly through the

52 oxidation of SO₂. Sulfur dioxide's lifetime in the atmosphere strongly depends on the oxidation
53 rate. The lifetime was shown to vary from up 48 hours in winter to around 13 hours in summer
54 based on a study performed with GEOS-Chem model simulations and observations (Lee et al,
55 2011). The deposition of SO₄²⁻ does not necessarily occur near the emission site or in the same
56 areas with high SO₂ concentrations. The wet deposition process is driven by precipitation and air
57 flow patterns in addition to sulfur chemistry. It is important to quantitatively attribute changes in
58 emissions to those in the deposition trends over downwind areas in order to characterize benefits
59 of regulatory controls.

60 The advent of satellite remote sensing has greatly aided in quantifying amounts of
61 various pollutants. In particular, remote sensing of SO₂ column amounts is performed using the
62 Aura satellite / Ozone Monitoring Instrument (OMI). This product has proved useful in locating
63 SO₂ sources and observing their changes in emissions (McLinden et al., 2016; Li et al., 2017a).
64 For example, a study using the previous OMI SO₂ product detected a 40% decline in SO₂ near
65 the largest coal power plants between 2005-2007 and 2008-2010, consistent with regulations on
66 emissions (Fioletov et al, 2011). The latest OMI product is based on a new retrieval technique
67 (Li et al., 2013; 2017b) that further reduces retrieval noise and artifacts, allowing for better
68 detection of sources. A study using this new OMI SO₂ products demonstrates good correlation (r
69 = 0.91) between reported emission rates and OMI-estimated emissions, and sources with
70 emissions greater than 30 kt/y can be detected (Fioletov et al., 2015), as compared with 70 kt/y
71 from the previous OMI products. Another study (Krotkov et al, 2016) indicates that from 2005-
72 2015, OMI column amounts of SO₂ decreased by up to 80% in the eastern United States due to
73 stricter pollution control measures.

74 The wet and dry deposition of SO₂ and its secondary SO₄²⁻ aerosol product are a
75 significant environmental issue, especially downwind of the source areas. In particular, acid

76 deposition is harmful for tree health and soil chemistry by depleting plant nutrient cations and
77 increasing acidity (Driscoll et al, 2001). Furthermore, much of the aerosol formed from gaseous
78 pollutants gets deposited in areas downwind of sources. A number of studies have been
79 published attempting to link the wet deposition with emissions and atmospheric transport
80 processes. Samson et al. (1980) performed a meteorological analysis based on air trajectories and
81 found little relationship between SO_4^{2-} and sulfur emissions. However, a later study by the same
82 group showed that the two could be explicitly linked in several areas while being unrelated in
83 others (Brook et al., 1994). Wet deposition was shown through modeling to have a statistically
84 significant relationship with SO_2 emission reduction due to policy changes in the late 1980s and
85 early 1990s (Shannon, 1999). An earlier study also estimated separation distances and
86 atmospheric transport for atmospheric SO_2 and SO_4^{2-} (Shannon, 1997). In the late 20th century,
87 locations in upstate New York, despite their relatively low local SO_2 concentrations, experienced
88 acid rain and deposition problems. Emission reductions upwind have been found to have a linear
89 relationship with SO_4^{2-} aerosol concentrations in several locations in the area (Dutkiewicz et al,
90 2000). The study used NOAA Hybrid Single Particle Lagrangian Integrated Trajectory
91 (HYSPLIT) model (Stein et al, 2015) to track air trajectories to identify major source regions of
92 SO_4^{2-} in Ontario and the Ohio River Valley. In particular, lakes in the Adirondack region in
93 upstate New York have shown decreases in SO_4^{2-} concentrations and reasonable correlation ($r^2 =$
94 0.58) between SO_2 emission in the eastern United States and wet deposition changes downwind,
95 at Whiteface Mountain and Huntington Forest (Driscoll et al, 2003).

96 Several more recent works have also focused on how meteorology plays a role in aerosol
97 transport and deposition. One such study incorporated methods such as the Positive Matrix
98 Factorization (PMF), Conditional Probability Function (CPF) and the Potential Source
99 Contribution Function (PSCF) to attribute sources of $\text{PM}_{2.5}$ in the Pittsburgh, PA area through

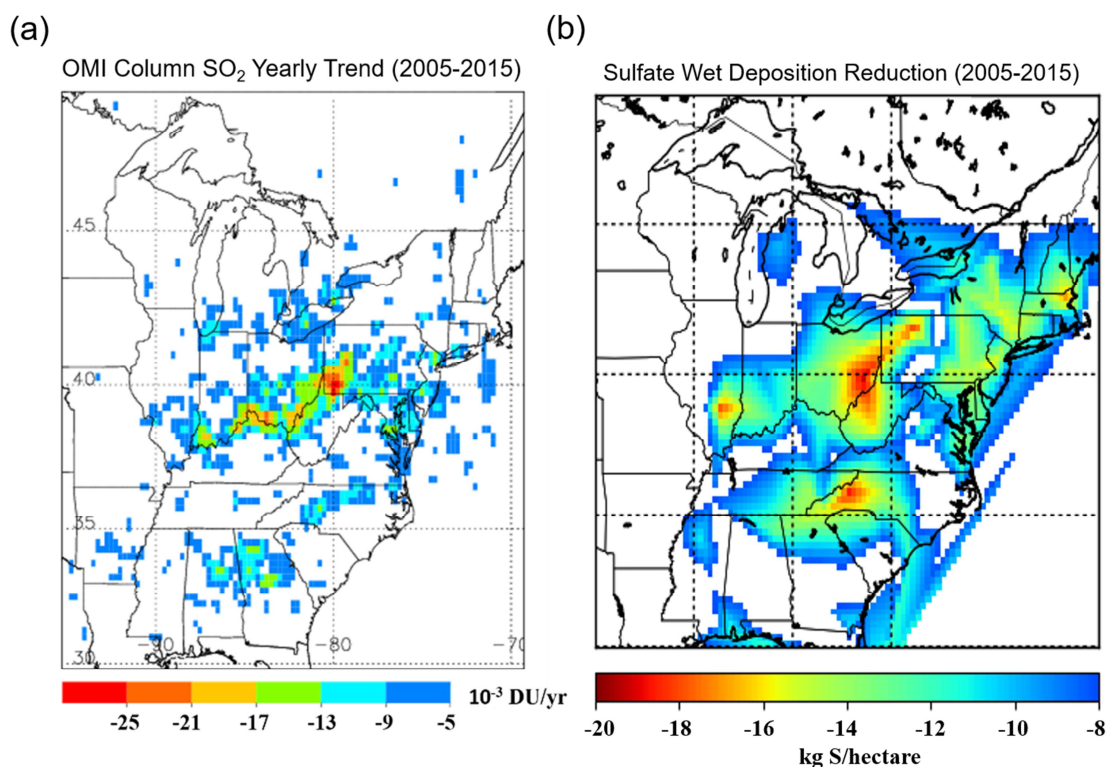
100 trajectory modeling (Peckney et al, 2017). In another study (Begum et al, 2002), the PSCF
101 method was employed to identify the source location of a Quebec forest fire from $PM_{2.5}$
102 measurements. An earlier study modeled the transport of sulfur species from source to the
103 receptor sites in Southern California (Gao et al, 1993). Other localized trends in particulate
104 matter have also been addressed, particularly in the I-95 corridor of the Mid-Atlantic region. A
105 study incorporating modeling and observations showed contributions from both regional and
106 local sources within 100 km of the Baltimore-Washington, D.C. corridor and that the local
107 contribution to $PM_{2.5}$ mass varies seasonally, from >60% in winter to <30% in the summer (Chen
108 et al., 2002).

109 Similar studies were performed for sites in Wisconsin, where enhanced SO_4^{2-} and nitrate
110 concentration originated from air arriving from potential sources near the Ohio River (Heo et al,
111 2013). Recent work incorporated observations of satellites such as GOME and SCHIAMACHY
112 along with GEOS-Chem transport model to constrain global reactive nitrogen deposition rates
113 and trends since 1996 (Geddes et al, 2017). While a considerable number of studies have
114 quantified source-receptor relationships in regards to atmospheric deposition for multiple sites,
115 less work has been done with more recent deposition data and satellite data. This study aims to
116 take advantage of the spatial consistency of OMI column SO_2 measurements, ground based SO_2
117 observations and SO_4^{2-} deposition. Between 2005 and 2015, many sites in the eastern U.S. saw
118 substantial reductions in wet deposition of SO_4^{2-} . But it is not yet clear which sources of
119 atmospheric SO_2 contributed most to these reductions in deposition and whether there is
120 significant difference in between summer and winter. This study aims to shed some light on
121 these important questions. The methodology and analysis presented in this study can be
122 applicable to other areas, especially those experiencing significant pollution and deposition
123 problems.

124 2 Methods:

125 2.1 Data

126 The Ozone Monitoring Instrument (Levelt et al., 2006) has been providing remote sensing
127 products of gaseous pollutants, including sulfur dioxide since 2004. SO₂ column amount is
128 retrieved using an algorithm based on principal component analysis of radiances measured by the
129 satellite (Li et al., 2013) that significantly reduces the retrieval noise and artifacts. The SO₂ data
130 from OMI has been used in a number of previous studies, particularly those on SO₂ emission
131 source regions. For the purposes of this study, Level 3 column SO₂ data (NASA GES-DISC,
132 2017) was used to derive the trend over the eastern United States for the period of 2005-2015.
133 This data has a spatial resolution of 0.25° latitude by 0.25° longitude, and is limited to scenes
134 with relatively small cloud fraction (< 0.3). To reduce the impacts of extreme values on the
135 average trend, negative outliers (< -2σ) were filtered out in the calculation of the averages,
136 following Zhang et al. (2017). In addition, to remove the effects of extreme values likely caused
137 by transient volcanic plumes, values greater than the 99th percentile of the SO₂ values in the U.S.
138 domain were excluded from the averaging process (McLinden et al., 2016). The OMI column
139 SO₂ ten-year trend (Figure 1a) was obtained by calculating the three year running mean from
140 2005 to 2015 and deriving to a linear trend with an annual time step. This trend also highlights
141 the areas that have experienced reduced emissions in the last ten years.



142

143 Figure 1: (a) Annual trend in OMI Column SO₂ in the eastern United States calculated using
 144 yearly averages, from 2005 to 2015 (b) Change in wet SO₄²⁻ deposition between 2005 and 2015
 145 over the same domain and time period, based on NADP deposition measurements.

146 Sulfate wet deposition data was obtained from the National Atmospheric Deposition Network
 147 (NADP). This network, consisting of over 150 monitoring sites nationally, collects rainwater
 148 samples and analyzes them for various chemical species (Lamb et al, 2000). Total SO₄²⁻ wet
 149 deposition is estimated annually for each station, as end of year totals with the deposition given
 150 in units of kg S/ha. Due to the non-gridded nature of the data, we interpolated the annual
 151 deposition to a regular grid, using Inverse Distance Weighting (IDW) and Kriging interpolation
 152 methods, shown to be most efficient for calculating special deposition patterns (Qu et al, 2016).
 153 A ten-year trend and net reduction (Figure 1b) in SO₄²⁻ over the entire U.S. domain (CONUS)
 154 was calculated for each grid box in the same way as for the SO₂, to provide SO₂ and SO₄²⁻ trend

155 values for each grid square. While the NADP does not have ideal coverage, there are sufficient
156 active sites in the Eastern U.S. to create a gridded field with spatial interpolation (Figure 2a),
157 albeit with some error.

158 Another dataset employed in this study is from the Environmental Protection Agency
159 (EPA) Air Quality System (AQS). This network provides hourly and daily ground-based
160 measurements of SO₂. For the purposes of this study, AQS data was used in the PSCF analysis,
161 described later in this section. Dry deposition, a variable percentage of total SO₄²⁻ deposition
162 (Vet et al, 2013), is measured by the CASTNET network (U.S. EPA CASTNET, 2017). Our
163 primary focus in this study was on wet deposition, since wet deposition is more dependent on
164 weather and precipitation tracks than is dry deposition. At sites in our domain west of the
165 Appalachians, dry deposition contributed >50 % of the S deposition, but east of the mountains
166 wet deposition dominated (NADP, 2016) for the study period. The deposition trends discussed in
167 the methodology and results will refer to wet deposition unless otherwise stated. Lastly, we used
168 some hourly SO₂ emission data obtained from power plant continuous emission reporting
169 systems (CEMs) through the EPA (U.S. EPA, 2017).

170 2.2 Trajectory Analysis

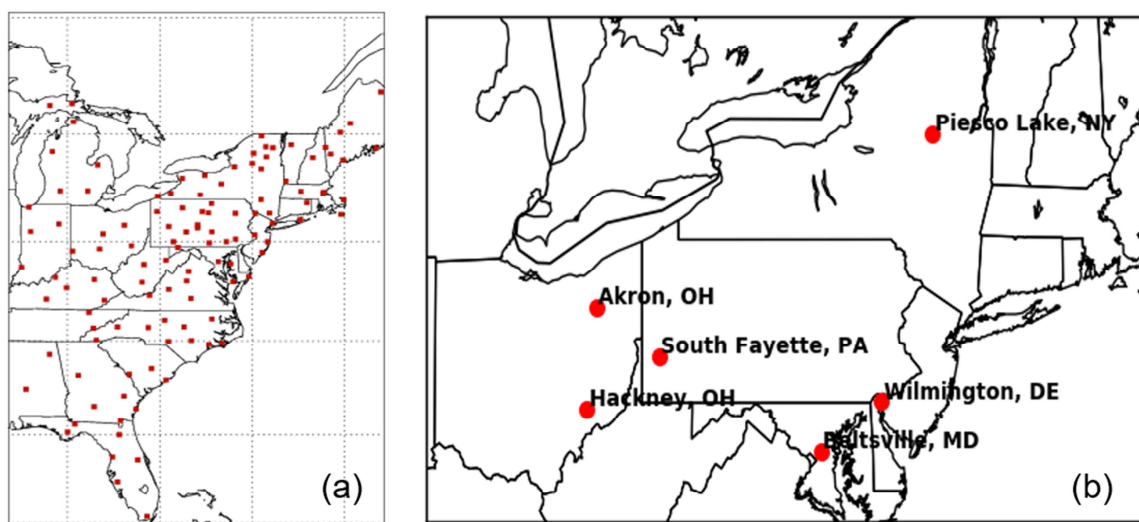
171 A trajectory analysis was used to diagnose the possible origins of the air containing elevated
172 amounts of SO₂ at various sites in the Eastern United States. Airflow patterns revealed by this
173 analysis can help to establish the link between the trends in SO₂ emissions and SO₄²⁻ wet
174 deposition. The sites chosen for the trajectory analyses (Figure 2b) are in the AQS network with
175 available SO₂ in-situ data, as well as a corresponding NADP site nearby with deposition data.
176 The five sites chosen were 1) Hackney, OH [81.670° W, 39.632° N], 2) Beltsville, MD [76.817°
177 W, 39.028° N], 3) Akron, OH [81.469° W, 41.0635° N], 4) South Fayette, PA [80.167° W,
178 40.3756° N] and 5) Wilmington, DE [75.558° W, 39.7394° N]. All of these sites had a

179 significant downward trend and at least 50% decrease in deposition between 2005 and 2015
 180 (Table 1). A site in upstate New York [74.500° W, 43.4336° N], Piesco Lake, was also
 181 considered due to a considerable downward 10-year SO_4^{2-} wet deposition trend in the region,
 182 however the in-situ SO_2 concentrations were too low to perform a meaningful trajectory analysis.
 183 The SO_2 at the this AQS site only exceeded 2.5 ppb 28 days in the winters and not once in the
 184 summers over a three year period.

Table 1: The 2005 and 2015 sulfate wet deposition amounts for the six initial case sites. Values were obtained directly from the annual NADP dataset for each site.

Site	SO_4^{2-} Wet Deposition 2005 (kg S /ha)	SO_4^{2-} Wet Deposition 2015 (kg S /ha)	% decrease 2005-2015
Hackney, OH	26.70	8.76	67.2
Akron, OH	22.08	11.08	49.8
Beltsville, MD	18.83	6.93	63.2
Wilmington, DE	19.41	5.57	71.3
South Fayette, PA	25.82	9.82	62.0
Piesco Lake, NY	19.04	7.93	58.3

185



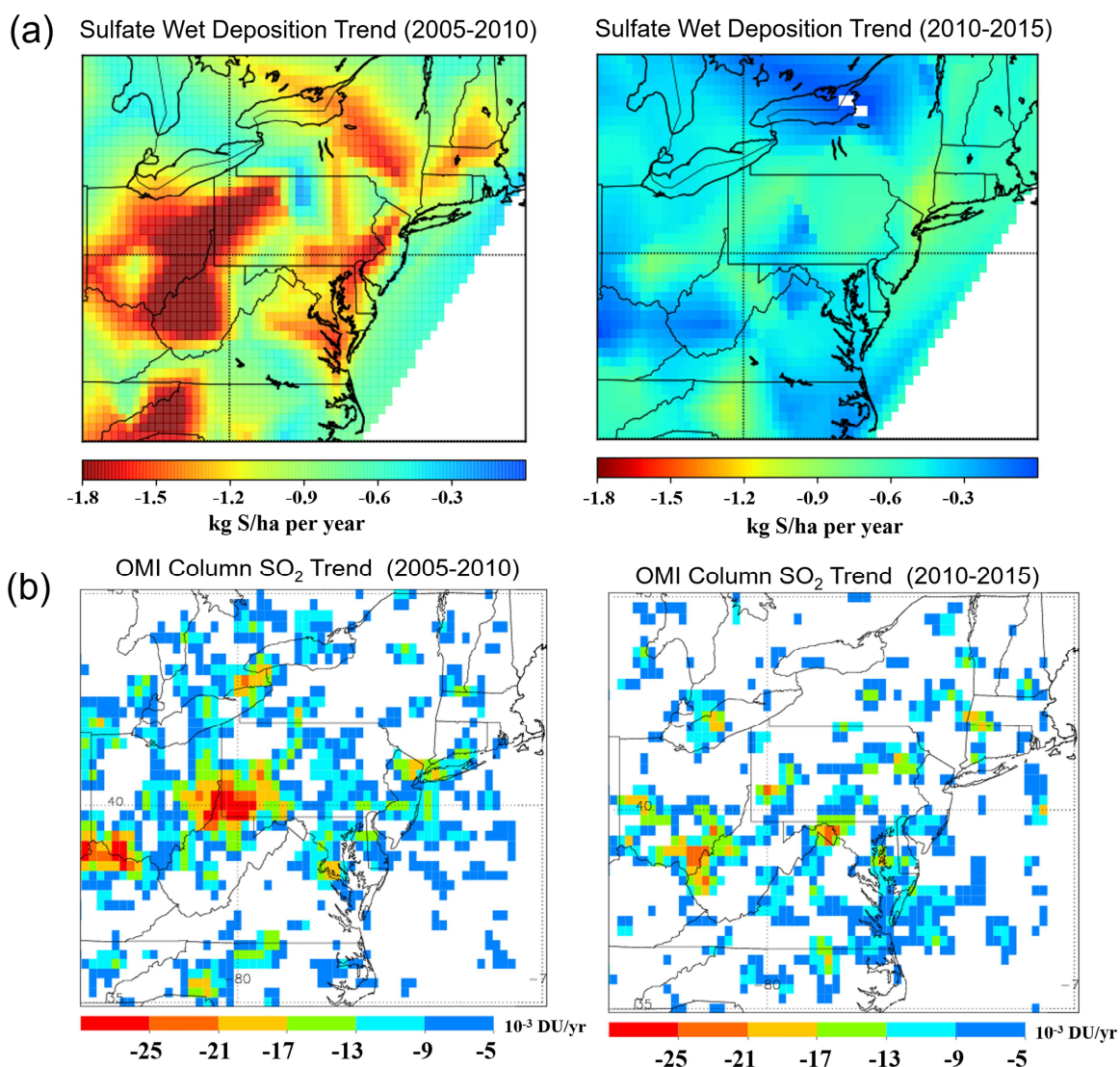
186

187 Figure 2: Locations of (a) observing sites in the NADP network, shown by the red squares and

188 (b) AQS sites initially chosen for the main analysis. These sites are in reasonably close proximity

189 to NADP sites. Refer to the text for the exact coordinates. The site in New York was removed
190 from the analysis due to SO₂ concentrations frequently below the detection despite having a
191 considerable sulfate wet deposition trend.

192 The HYSPLIT trajectory model from NOAA (Stein et al, 2015) was used to calculate
193 back trajectories. Three day back trajectories were calculated each day using archived Eta Data
194 Assimilation System (EDAS) meteorological data at 40 km resolution. The HYSPLIT model
195 runs were initialized daily at 18Z near the overpass time of the satellite. The initialized height
196 was kept constant in the model runs at 500 m above ground level. A climatology of back
197 trajectories was obtained for each site by running daily 72-hour back trajectories for three
198 summers (JJA) and three winters (DJF), in the period 2006-2009. This period was selected
199 because larger downward trends in column SO₂ and SO₄²⁻ wet deposition occurred in 2005-2010
200 than in 2010-2015, as shown by trend maps for the two time periods (Figure 3). However,
201 changes in the average seasonal large-scale flow pattern are unlikely to be strongly dependent on
202 the period selected.



203

204 Figure 3: Annual trend for a) NADP sulfate wet deposition and b) OMI Column SO₂ for 2005-
 205 2010 (left) and 2010-2015 (right). The improvements in column SO₂ occurred at sites closer to
 206 the sources than did the improvements in deposition, but the trends are consistent.

207 2.3 Potential Source Contribution Analysis

208 The need for a trajectory and PSCF analysis stems from the fact that the spatial correlation
 209 between wet SO₄²⁻ deposition and OMI column SO₂ trends is overall fairly weak across the
 210 entire domain. The low R² coefficient (0.036) showed poor correlation between the two

211 normalized trends (Figure A.1). The method used to normalize the trends will be discussed
212 further in section 2.4. To link the trends, characteristic air patterns for a given location are needed
213 to understand the trends occurring in those locations. The calculated trajectories were obtained
214 for the purpose of calculating the probability of high concentrations of SO₂ coming from a given
215 grid box in the domain.

216 The Potential Source Contribution Function (PSCF) is defined as the number of trajectories
217 passing through a grid box carrying an amount of SO₂ exceeding a set threshold (*m*) divided by
218 the number of total trajectories going through that same grid box (*n*). Thus each grid box would
219 have its own PSCF value, between 0 and 1. The function is expressed as:

$$PSCF_{ij} = \frac{m_{ij}}{n_{ij}} \quad (1)$$

222 The subscript *ij* denotes a single grid box on the grid domain. The domain over which the
223 function was calculated was ±5 degrees latitude and ±7.5 degrees longitude from each site. The
224 domain size and location were chosen based on the typical distance covered by trajectories
225 within 72 hr. Based on the arithmetic mean and median concentrations of SO₂ recorded at each
226 of the sites over the three year period (Table 2), we chose a value of 5 ppb as the SO₂ threshold
227 for all of the base cases except for the winter South Fayette, for which the threshold was set at
228 7.5 ppb. These thresholds were kept constant throughout the entire analysis. A simple weighting
229 scheme was assigned for the calculation to remove the influence of low sample size (Pollisar et
230 al, 1999). The weighting was performed in order to eliminate the sample size issues, or
231 occurrences of low values of *n_{ij}*. For grid boxes with *n* < 8 trajectories, the PSCF value is
232 multiplied by a weighting factor of 0.07. Similarly, for grid boxes with 8-16 and 16-24
233 trajectories, we use a weighing factor of 0.45 and 0.7, respectively. These new values are the
234 weighted potential source contribution functions (WPSCF) and were calculated for each of the

235 five sites for JJA and DJF. The weighted scheme is arbitrary and varies across literature,
 236 however the one used here is very similar to a study to identify potential source regions of $PM_{2.5}$
 237 in Beijing using the same type of back-trajectory analysis (Zhang et al, 2015). Aside from using
 238 HYSPLIT to acquire trajectories and graphics generating scripts, we used a GIS-based software
 239 called Trajstat to analyze the trajectories and PSCFs. This software was originally produced for
 240 statistical analysis of air pollution data and includes basic geographic map layers and trajectory
 241 file conversion capabilities (Wang et al, 2009).

242

Table 2: Mean and median winter SO_2 concentration as measured by the five AQS sites over the 2006-2009 period. These metrics were used to choose a threshold value for the PSCF analysis.

Site	Mean(ppb)	Median (ppb)
Akron, OH	5.15	4.3
Hackney, OH	6.62	4.9
S. Fayette, PA	7.62	6.9
Beltsville, MD	4.35	6.3
Wilmington, DE	5.14	4.8

243

244 **2.4 Normalized Trends**

245 To factor in the effect of the PSCF on the trends, we transformed both trends to the same,
 246 normalized scale. The SO_4^{2-} wet deposition trends were normalized to a scale of 0 to 1 with the
 247 grid box having the highest downward trend assigned a value of 1 and the a grid box with the
 248 highest positive trend assigned a value of 0 (eq. 2). The cases of an upward 10-year trend in the
 249 deposition were very few in the eastern domain and thus did not influence the outcome. The
 250 column SO_2 trend over the entire domain was also normalized the same way (eq. 2):

$$x_{ij,norm} = \frac{X_{ij} - \min(X)}{\max(X) - \min(X)}, \quad (2)$$

252 Where x is the normalized trend value for a given grid box, X_{ij} is the raw trend for the same grid
 253 box and X is the set of gridded trend values for the entire domain. Multiplying the normalized
 254 trends result by the PSCF produces a relative product value that describes the relative
 255 contribution of the air coming in that grid box to the trend. A grid box with both a high PSCF
 256 and large downward wet deposition trend would indicate that air arriving from there has seen
 257 significant reductions in sulfur over the years, thus contributing to the decrease in wet deposition
 258 at the receptor locations. To relate the NADP trend to OMI observations, the normalized 10 year
 259 trend in column SO_2 was added into the calculation.

$$z_{ij} = \text{norm}(\text{SO}_2 \text{ Trend}) \times [\text{WPSCF} \times \text{norm}(\text{SO}_4^{2-} \text{ Trend})] \quad (3)$$

260 This product value helps to identify, for a given receptor site, upwind source locations that not
 261 only frequently influence the site through transport and also have large decreases in SO_2
 262 emissions between 2005 and 2015 according to OMI. All three terms are necessary since the
 263 deposition trend, emissions and transport are accounted for. Using only the normalized SO_2 trend
 264 would only indicate contributions to decreasing SO_2 at the site, rather than deposition. Likewise
 265 using only the normalized SO_4^{2-} wet deposition trend, the influence of emission reductions is
 266 removed from the contribution. A percent contribution was then calculated for each grid box
 267 through the summation of individual grid box values and dividing each individual value by the
 268 total.

$$\% \text{ contribution} = \frac{z_{ij}}{\text{sum}(z_{ij})} \times 100\% \quad (4)$$

270 Thus this new value expresses the normalized contribution of a particular grid box

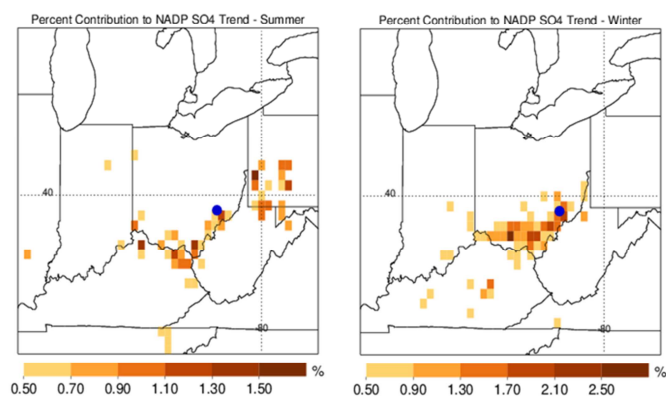
271 to the SO_4^{2-} wet deposition trend at the AQS or NADP site, relative to the domain. This provides
272 a quantitative assessment of the trend data relationship.

273 **3. Results and Discussion**

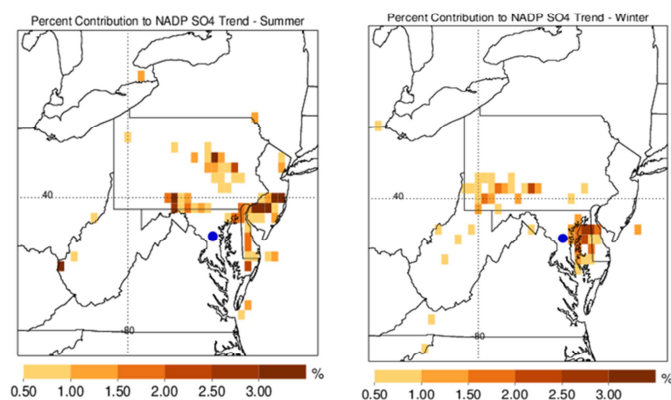
274 **3.1 Percent contributions**

275 This section describes the qualitative and some quantitative aspects of the grid boxes that
276 contribute to wet deposition trends at five different sites. Figures 3 and 4 show grid cells in the
277 domain with a color representing the final percent contribution value calculated with equation 4.
278 We aim to show the specific grid boxes which had the most contribution in the domain to the wet
279 deposition trend at the receptor site, as well as the cumulative contribution at various distances
280 from the site through summations of the percent contribution values.

(a) *Hackney, OH*



(b) *Beltsville, MD*



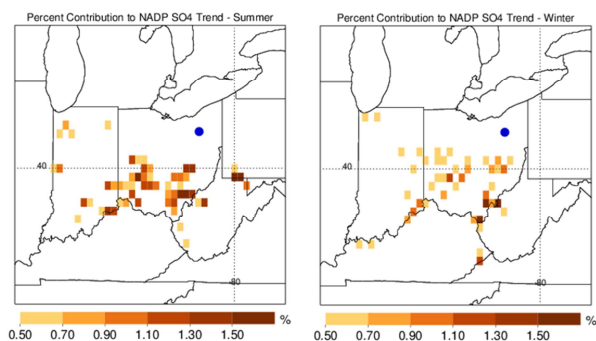
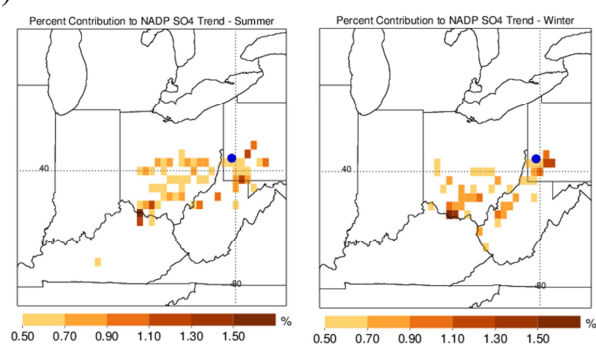
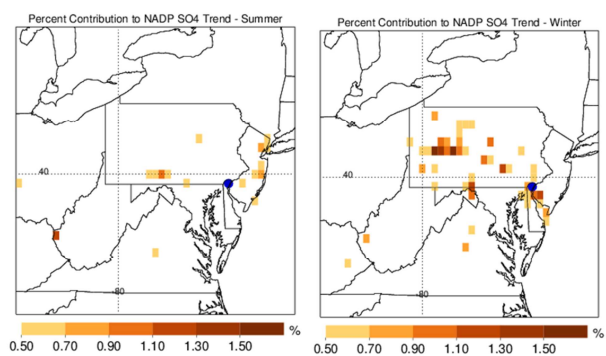
281

282 Figure 4: Percent contribution for each grid box in the domain with only values above 0.5%.

283 Shown for (a) Hackney, OH and (b) Beltsville, MD sites in JJA (left) and DJF (right). The

284 observation sites are marked with a blue dot.

285

(a) *Akron, OH*(b) *South Fayette, PA*(c) *Wilmington, DE*

286

287 Figure 5: Percent contribution for each grid box in the domain with only values above 0.5%.

288 Shown for (a) Akron, Ohio, (b) South Fayette, PA and (c) Wilmington, DE AQS sites in JJA

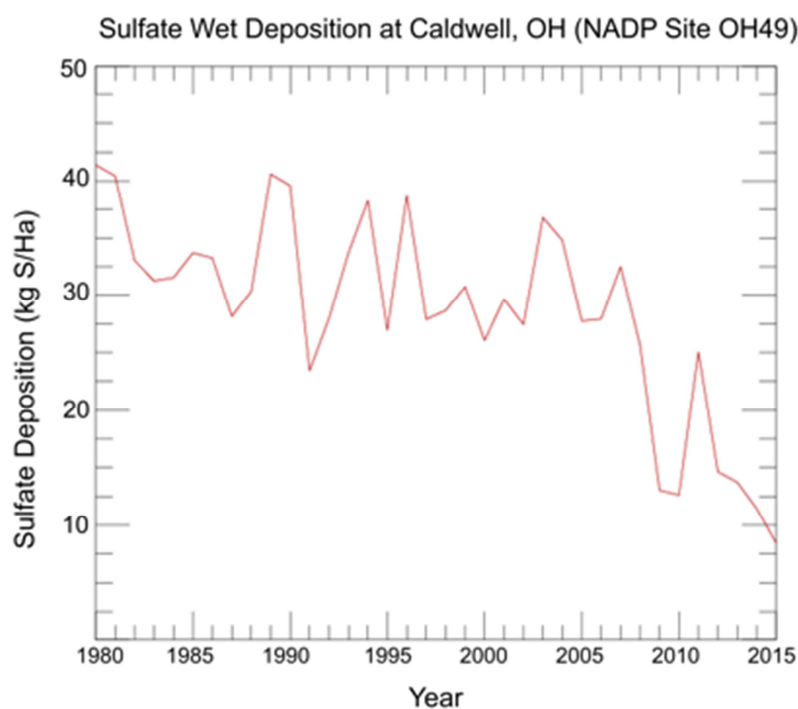
289 (left) and DJF (right). The observation sites are marked with a blue dot. Note that only values

290 greater than 0.5% are colored.

291

292 *Hackney, OH*

293 Due to its proximity to numerous sulfur emitting coal-fired power plants, the Hackney, OH AQS
294 site shows high concentrations of SO₂ with average daily value of around 7 ppb and often
295 exceeding 20 ppb in winter. The corresponding NADP site for this area is in Caldwell, OH (Site
296 ID OH49), ~18 km away. We would expect similar characteristic deposition and trajectory
297 patterns for the two locations given the flat terrain and proximity to the same SO₂ sources. In
298 wintertime (DJF), wet deposition trend at the Caldwell NADP site is driven by the dominant
299 southwesterly flow and high outputs of emissions upwind near the Ohio River (Figure 4a). The
300 observed annual wet deposition at the Caldwell site decreased from 23.35 kg S/ha in 2005 to
301 8.76 kg S/ha in 2015 according to the NADP dataset. The wet deposition has significant year-to-
302 year variability (Figure 6), however, the overall 10-year trend from 2005 to 2015 was downward.

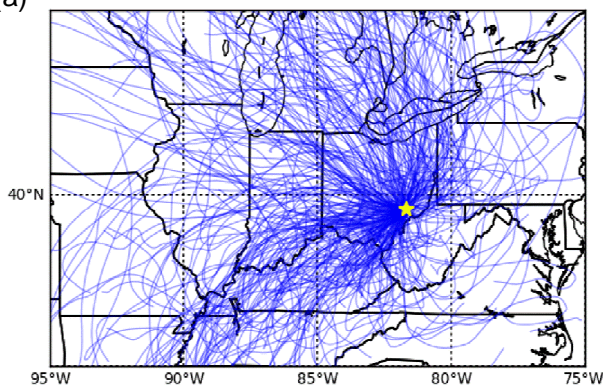


303

304 Figure 6: Sulfate Wet Deposition amounts at Caldwell, OH NADP site, shown as a time series
305 from 1980 to 2015. The plotted data is from the NADP network at the OH49 site [39.7928 N,
306 83.5311 W]

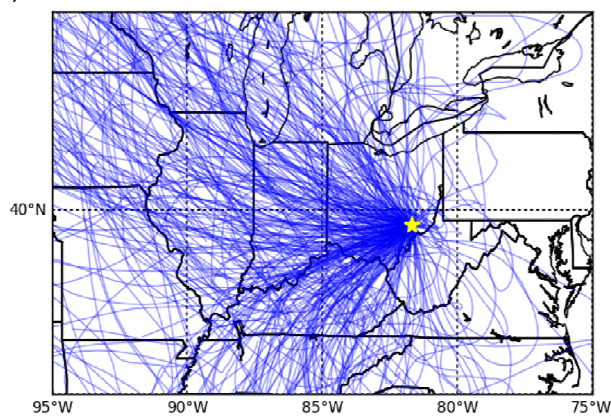
307 Qualitatively, the area with the colored grid boxes in southern Ohio largely contributed to the
308 decreasing deposition (Figure 4a). In summer (JJA), major areas in southwestern PA with large
309 SO₂ columns somewhat contribute to the observed trend at the Hackney site, however less so
310 than the sources along the Ohio River. The trajectory climatology for this site (Figure 7) shows a
311 clear seasonal change in direction trajectories indicating that emission reduction in the west have
312 likely contributed to the majority of the observed trend at the site.

(a) Hackney, OH AQS Site JJA Trajectories (2008-2009)



313

(b) Hackney, OH AQS Site DJF Trajectories (2006-2009)



314

315 Figure 7: Map of (a) summer (JJA) and (b) winter (DJF) trajectory climatology for 2006-2009 at
316 Hackney, OH. The yellow star shows the location of the site and the blue lines are the individual
317 72 hour back trajectory for each day, initialized at 18Z using the HYSPLIT model.

318 *Beltsville MD*

319 The Beltsville, MD site experienced a downward SO_4^{2-} wet deposition trend, especially in the
320 years 2008-2012, and has two primary regions that contributed to the 10-year decrease. The
321 Southwest PA region shows the greatest cumulative percent contribution which implies that wet
322 deposition has dropped due to the decrease in sulfur emissions in Pennsylvania. However, we
323 also see a signal to the east of the site in the PSCF and contribution map (Figure 4b). While the
324 dominant trajectory is from the northwest in winter, air can occasionally arrive from the east in
325 both seasons. In summer, wind direction is more variable compared to winter, as indicated by the
326 trajectories from HYSPLIT (Figure 8). Just before the turn of the decade in 2010, Maryland's
327 Healthy Air Act led to cuts of sulfur emissions of 80-85% from levels in the early 2000s (He et
328 al., 2016). While most of the contribution is due to decreased emissions to the west, it is probable
329 that local emission controls have also played a role in decreasing SO_4^{2-} deposition in the general
330 vicinity. The case for this site will be further investigated in section 3.3.

331

332

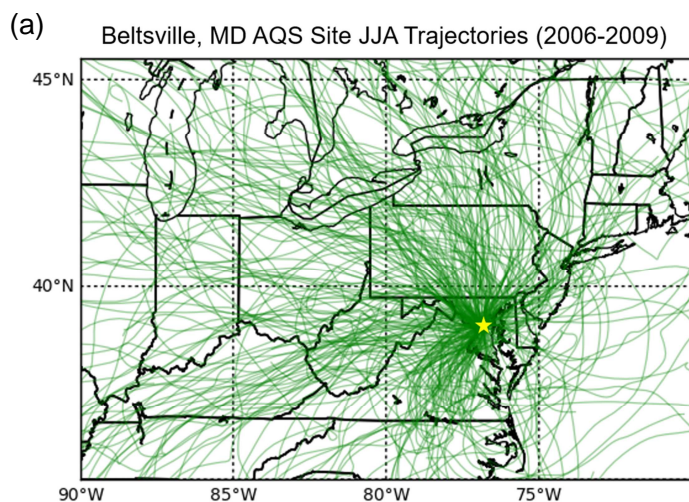
333

334

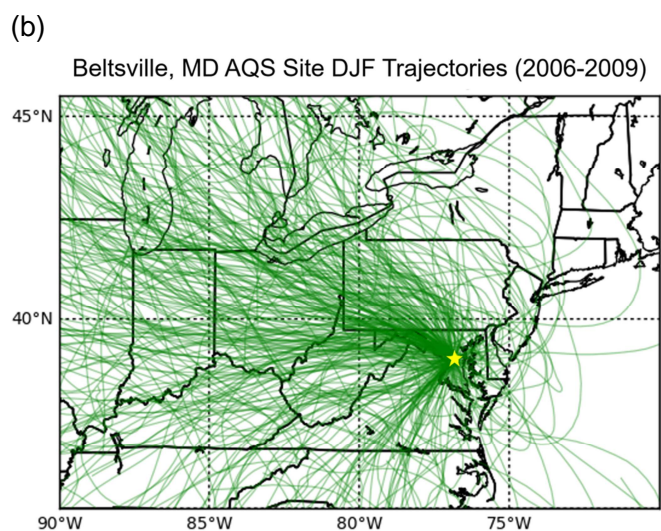
335

336

337



338



339

340 Figure 8: Same as Figure 7 but for Beltsville, MD AQS site. The trajectories are denoted by
341 green lines in this figure

342 *Akron, OH*

343 Sources to the south and southwest dominate the wet deposition trend for the Akron, OH (Figure
344 5a). Most of the grid cells with a non-negligible percent contribution (greater than 0.5 %) are
345 located near major SO₂ sources, approximately 100-300 km away from Akron in both winter and

346 summer. The percent contributions show fewer grid boxes with contributions over 1.5% in
347 winter as the contribution is spread out over larger number of grid boxes, especially those further
348 away. This is reflected by higher emissions, generally higher wind speed and longer trajectory
349 distance within the 72 hours in wintertime. In summer months there is also signal from southwest
350 PA with over 1.5% contribution for two grid cells in that region.

351 *South Fayette, PA*

352 The AQS site in South Fayette, PA had the highest median in-situ SO₂ amounts of the five sites
353 reported in the 2006-2009 period for both winter (~7.0 ppb) and summer (~3.5 ppb), whereas in
354 Hackney those median amounts were 5.4 and 2.7 ppb respectively. Sulfate deposition is affected
355 by local sources, but the PSCF analysis also shows elevated SO₂ concentrations arriving from the
356 east and southwest, near the sources along the Ohio River. During summer, there is slightly more
357 contribution from the east, indicating a shift from a predominantly western zonal flow that
358 occurs during winter. However, the seasonal difference in the contribution appears to be smaller
359 than at other sites. The highest percent contributions in both seasons are from southern Ohio and
360 just to the east of the site (Figure 5b), which indicates the presence of sulfur emission sources. In
361 this sense, the site is quite similar to the patterns in Hackney, OH, except it is more affected by
362 the local power plants to the east in PA.

363 *Wilmington, DE*

364 For the Wilmington, DE site (Figure 5c), the region contributing the most in winter to the
365 deposition trend is from upwind in Pennsylvania, which is home to several large power plants.
366 As shown by OMI, the region had a strong decrease in column SO₂. Given the winter trajectory
367 pattern, it follows that any reductions in Pennsylvania benefitted the Wilmington area in terms of
368 deposition amounts. In summer, there is not much signal from any particular area, with isolated

369 grid boxes in the New York area and in southern PA. It is reasonable to assume that most of the
370 decrease in annual SO_4^{2-} wet deposition were due to large decreasing trend in winter SO_2
371 concentrations over upwind areas to the west. While there may have been some minor summer
372 contributions as well, their magnitude were not as great as in winter. This shows an absence of
373 SO_2 source near the site and that a stronger wintertime flow pattern is needed to have impacts on
374 the deposition trends.

375 **3.2 Contribution Distributions by Distance**

376 We extend the analysis above by calculating the total percentage contribution to trend observed
377 at a receptor site from all grid boxes within a certain distance from the site. Distances of 50, 100,
378 200, 300,400, 500 and 1000 km were used in the analysis. The calculation was performed by
379 creating a circle with a radius of the distance from the site and summing up the contribution of
380 all grid boxes that fall within the circle. This process leads to cumulative distributions of total
381 contribution moving away from the site. This would help in diagnosing if the wet deposition at
382 the site is primarily driven by local or upwind sources and the direction from which the sulfur is
383 arriving at the site.

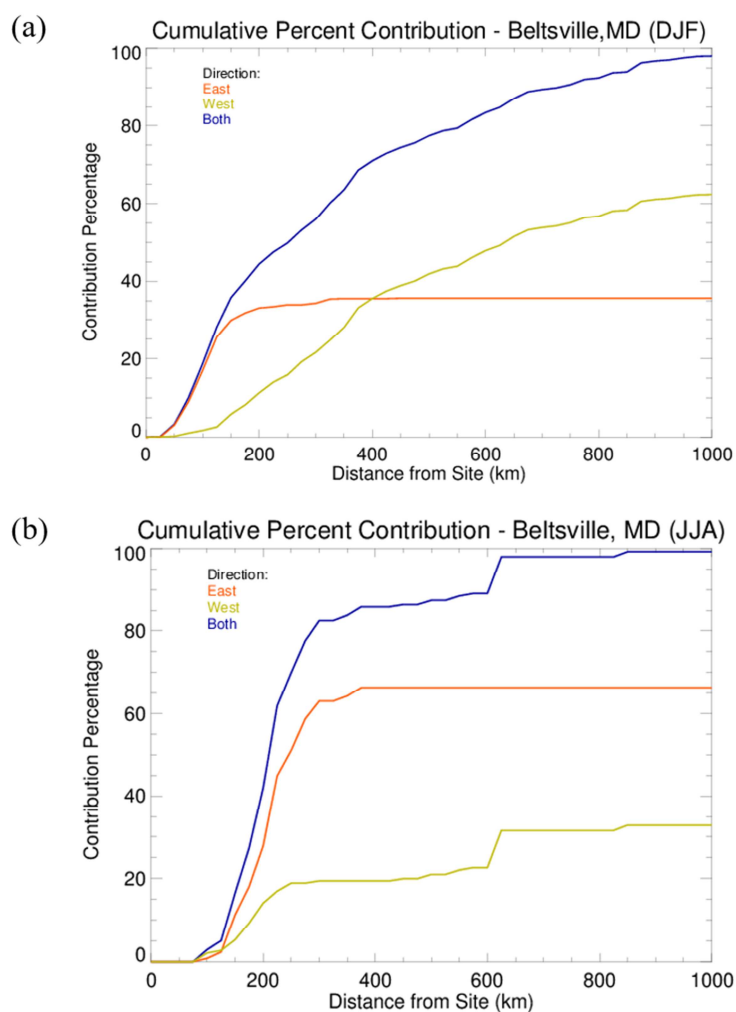
384 We calculated a cumulative contribution for two sites with significant climatological and
385 geographical differences, Beltsville (Figure 9) and Hackney (Figure 10), for summer and winter
386 seasons.

387

388

389

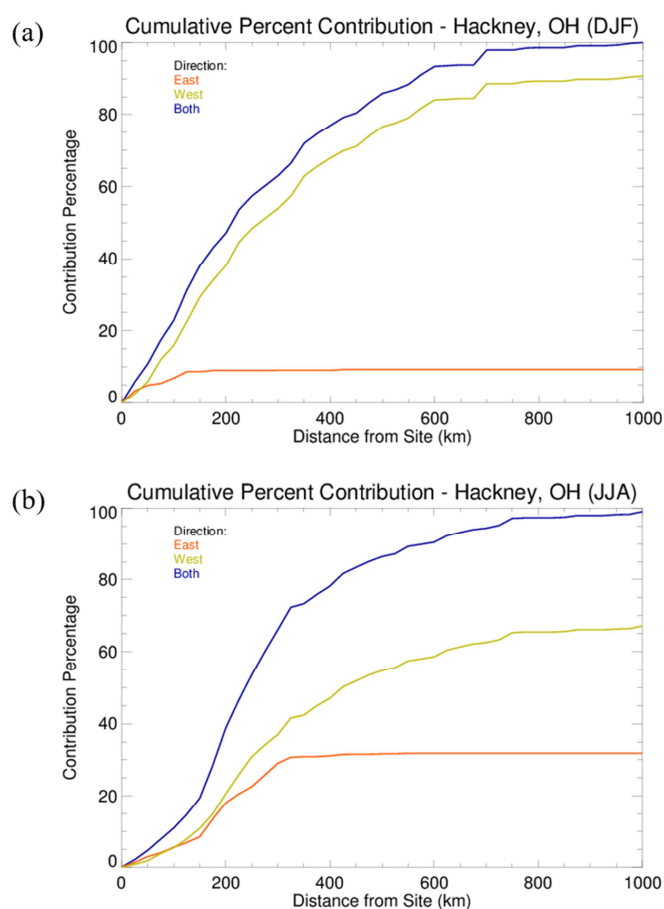
390



391

392 Figure 9: The cumulative percentage of contribution to the SO_4^{2-} -wet deposition trend at the
393 Beltsville NADP site, from areas within a given radius from the site (x-axis) for (a) winter and
394 (b) summer. The orange, green and blue lines represent contributions from locations with a
395 longitude east of the site, west of the site and all locations within the radius respectively.

396



397

398 Figure 10: Same as Figure 9 but for the Hackney AQS site.

399 *Beltsville, MD*

400 For the Beltsville site, half (50%) of the sulfur contributing to the ten-year wet deposition trend
 401 is linked to SO_2 observed within a 300 km radius in both winter (Table A.1) and summer (Table
 402 A.2). However, more contribution comes from locations over 300 km away in winter (44%) than
 403 in summer (17.5 %), showing that the lifetime and transport distances are generally greater in
 404 winter. The lower in-situ SO_2 amounts in summer than in winter are consistent with the fact that
 405 the largest SO_2 emitting power plants in the domain are more than 300 km away. Higher
 406 contribution values come from several grid boxes closer to the site in the Beltsville, MD case
 407 (within 100 km), yet the accumulated contribution in the southwest PA region has arguably more

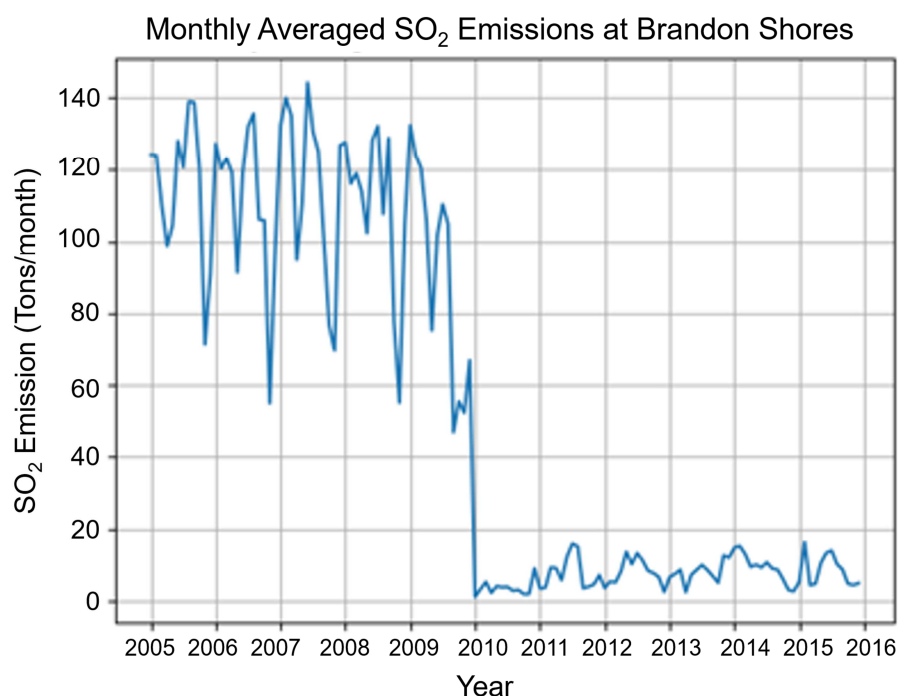
408 effect on the deposition trend. This is evidenced by sources more than 300 km to west of
409 Beltsville, MD that contribute more than 50% of the SO_4^{2-} . The result shows the benefit in
410 reducing emissions upwind in western PA and eastern Ohio, as the decrease has led to a
411 downward deposition trend in addition to improved SO_2 levels in the second part of the study
412 period. In summer, 83% of the contribution comes from within 300 km, with roughly 63% of this
413 coming from the east of the site. This indicates that summer transport distance is short and
414 pollutants are less likely to reach from beyond 500 km away as they do in winter.

415 *Hackney, OH*

416 In winter, while the total contribution from within 300 km (63%) is similar to summer for this
417 site, 54% of it is from the west (Table A.3). For summer, roughly 66% of the contribution is
418 from within 300 km of the site, with 29% of it from the east and 37% from the west (Table A.4).
419 While more of the contribution is from the west, the eastern component indicates that some of
420 the SO_4^{2-} originates from areas to the northeast of the site in PA in addition to areas to the
421 southwest of the site. Areas within 100-200 km from the site, contributed to about 24% and 27%
422 of the SO_4^{2-} wet deposition trend in winter and summer respectively, meaning the emission
423 source within that radius are more or less contributing the same in both seasons relative to the
424 rest of the domain. This is a different characteristic from Beltsville, MD since for Beltsville more
425 contribution came from further distances in winter and was not as greatly affected by SO_2
426 sources within 200 km of the site. Due to proximity of this site to some of the sources, it is
427 possible that the SO_2 from these sources was not resolved in the trajectory analysis with only 40
428 km resolution of the meteorology data. Over all distances, the western component dominates in
429 both winter and summer with roughly two thirds coming from the west in winter and 90% in
430 summer. This indicates the dominance of the climatological westerlies over source proximity and
431 deposition processes.

432 3.3 Case study on the impact of the Maryland Healthy Air Act on deposition at Beltsville

433 Evidence exists that in the present day, much of Maryland's sulfur pollution problem has
434 previously originated upwind in Pennsylvania and Ohio River valley. However, it is interesting
435 to assess the impact of local statewide regulations. The Brandon Shores power plant is one of the
436 biggest emitters of sulfur dioxide in Maryland, especially before the enactment of the Healthy
437 Air Act of 2010. The plotted average monthly emissions show that the facility cut its SO₂
438 emissions by over 80% post 2009 (Figure 11).

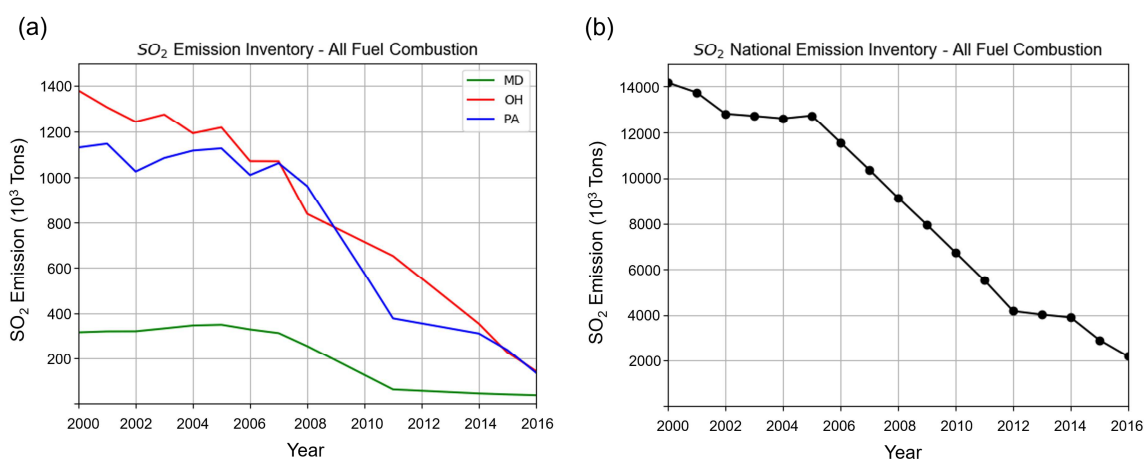


439

440 Figure 11: Monthly averages of hourly SO₂ emissions from the Brandon Shores power
441 generating facility, located just to the south of Baltimore, MD. The data were obtained from
442 Continuous Emission Monitoring Systems (CEMs) and are distributed by EPA's Air Markets
443 Program database.

444 Maryland state emission inventories (Figure 12a) also show roughly 80% drops in SO₂ emissions
445 between 2005 and 2015 in the fuel combustion sector, which includes power plant emissions.

446 There is a 78% drop in 2007-2012 and 45% drop for 2005-2009, indicating that Maryland cut
 447 more of its emissions in 2008-2012. At the same time, emissions have been decreasing
 448 consistently in Ohio and Pennsylvania, as well as nationally (Figure 12b). The trends for SO_4^{2-}
 449 and SO_2 are also of greater magnitude in 2005-2010 than in 2010-2015 (Figure 3), which aligns
 450 with emission trends and the enactment of the Healthy Air Act.

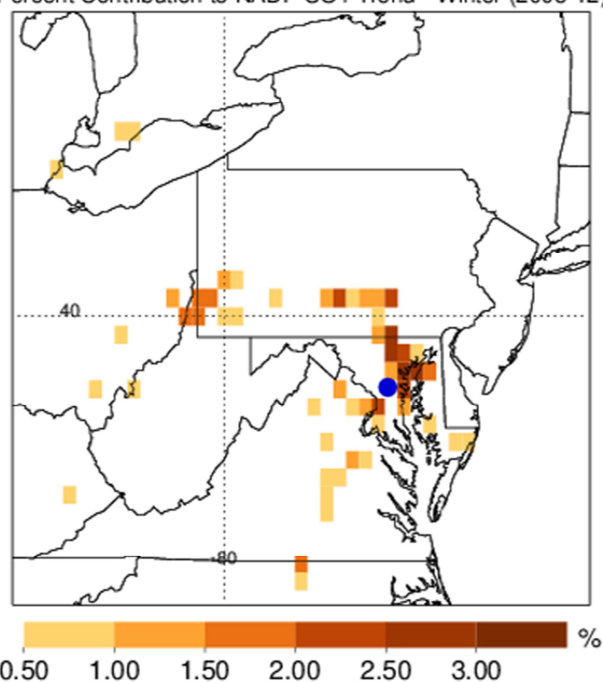


451
 452 Figure 12: The SO₂ emission inventory for (a) three states: MD, PA and OH and (b) the entire
 453 United States. Only the total values for the fuel combustion sector, which includes primary
 454 power plant emissions, are included. This sector is the dominant portion of the inventory and
 455 accounts for over 80% of the total. Emission inventory data can be found on the EPA Emission
 456 Inventory site: [https://www.epa.gov/air-emissions-inventories/air-pollutant-emissions-trends-](https://www.epa.gov/air-emissions-inventories/air-pollutant-emissions-trends-data)
 457 data

458 Using the same PSCF analysis method as above, we were able to identify contributions to the
 459 SO_4^{2-} sulfate wet deposition trend for 2008-2012 by using the trend and PSCF corresponding to
 460 this time period only. As seen in Figure 13, there is noticeably larger total contribution from
 461 areas close to the site than farther away. There is also a difference between the original 10-year
 462 case and this four-year time period in that the grid boxes directly to the northwest (Baltimore

463 area), contribute slightly higher from 1-1.5% in the 10-year case to 2-3% for 2008-12. The
 464 results here show that the state legislation may have had a positive impact in reducing sulfate
 465 SO_4^{2-} deposition at Beltsville.

Percent Contribution to NADP SO₄ Trend - Winter (2008-12)



466
 467 Figure 13: Percent contribution to the Beltsville, MD winter wet deposition trend for 2008-2012.
 468 The same procedure was used as in the other maps, except with a 2008-2012 winter trajectory
 469 climatology and PSCF

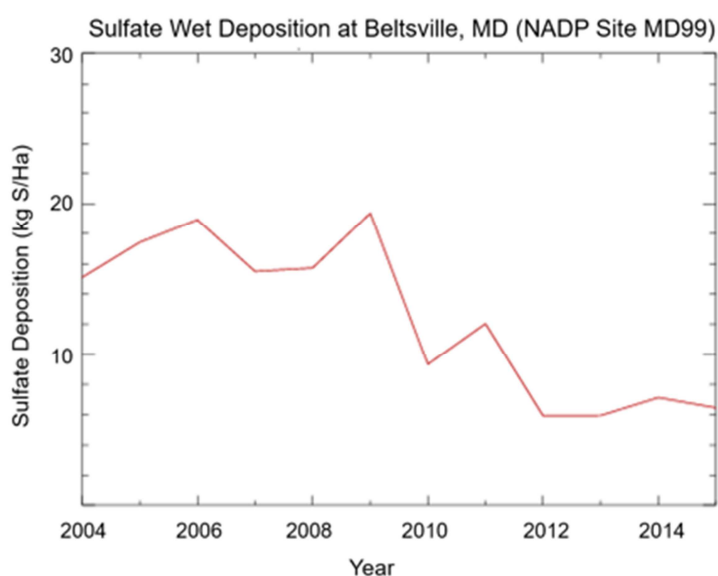
470 This result can also be related to the specific dry and wet deposition amounts occurring in
 471 Beltsville over the years. The data in Table 3 indicates that dry SO_2 and SO_4^{2-} deposition have
 472 decreased overall from 2005 to 2015. The decrease is better seen in the SO_2 than SO_4^{2-} between
 473 the first and second 5 years. The effect of cutting emissions at Brandon Shores has clearly
 474 decreased local dry deposition of SO_2 . The result is less obvious in the dry SO_4^{2-} , although by
 475 2015, the deposition has dropped by almost 50%, from 1.12 to 0.59 kg S/ha. The fraction of total
 476 S deposition due to dry deposition of SO_2 has fallen by roughly a factor of two over this decade,

477 consistent with greater partition into sulfate (Shah et al., 2018). According to Figure 14, the
 478 steepest trend in wet deposition occurred from 2008-2012. The wet deposition end-of-year total
 479 for 2012 decreased to 8 kg S/ha from around 20 kg S/ha, reported at the end of 2009 (Figure 14).

Table 3: Flux of dry SO₂ and SO₄²⁻ at the Beltsville, MD site in the CASTNET network with the annual NADP wet deposition totals. The flux value can be seen as dry and wet deposition of SO₄²⁻ at the site. Several years of dry flux data were missing in the dataset.

Year	Dry SO ₂ Flux (kg S/ha)	Dry SO ₄ Flux (kg S/ha)	Wet SO ₄ Flux (kg S /ha)
2005	7.547	1.857	17.42
2007	4.296	1.777	15.49
2008	4.268	1.426	15.72
2009	3.112	1.005	19.36
2010	2.227	1.126	9.34
2011	1.361	1.048	12.04
2013	1.009	0.785	5.95
2014	1.410	0.706	7.14
2015	1.071	0.588	6.46

480



481

482

483 Figure 14: Sulfate Wet Deposition amounts at Beltsville, MD, shown as a time series from 2004
484 to 2015. The plotted data is from the NADP network at the MD99 site.

485 However, wet deposition is largely driven by the precipitation patterns and consequently
486 by air trajectory climatology. Given that only less than 25% of back trajectories arrive from east
487 of the site in winter, it is difficult to conclude that the drop in local emissions was the dominant
488 factor in the overall decreasing trend. Yet the effect is non-negligible and may have certainly
489 played a role as the steepest slope indeed occurred between 2009 and 2010. Thus we can
490 speculate that the signal associated with the contribution values to the east and northeast of the
491 site as well as the increase in percent contribution for the 2008-2012 four year period, are not
492 anomalies or artifacts of the method, but significant characteristics of the contribution to the wet
493 deposition trend in Beltsville between 2008 and 2012. The local and statewide emissions likely
494 only affected the short-term trends in deposition given the drastic changes in emissions, rather
495 than the long term deposition changes over a 10 year period. The latter is likely driven by a
496 systematic drop of emissions on a larger regional scale and consistent trajectories from the
497 northwest. Lastly we roughly estimate the SO₂ lifetime qualitatively from the contribution maps.
498 In general, there is indication that lifetime is less than 1 day in the summer, while in winter the
499 SO₂ gets carried 100-200 km more especially for the eastern sites. The latter indicates a longer
500 SO₂ lifetime in excess of 1-1.5 days in winter. This is consistent with the SO₂ lifetimes of 13 h
501 and 48 h for summer and winter respectively found by Lee et al., and may be due to seasonal
502 differences in oxidation rates; Shah et al. (2018) reported only 18% of SO₂ was regionally (over
503 the eastern US) oxidized to SO₄²⁻ in winter, but 35% of summer. As shown previously, SO₂ and
504 SO₄²⁻ deposition trends can appear in geographically different areas. Locations that have
505 drastically reduced their sulfur emissions can still have SO₄²⁻ deposition problems due to upwind

506 sources and likewise can benefit from the reduction of emissions from those areas. Thus, both
507 local and regional pollution controls are not only important for air quality but for the
508 environment since air trajectory patterns control the transport and deposition of chemical species.

509 **3.4 Method Limitations and Uncertainties**

510 Although the methodology presented in this study was used consistently for all sites, it did not
511 come without limitations or systematic errors. In this section we discuss potential sources of
512 error and uncertainty stemming from the methods and factors that were difficult to constrain in
513 this study.

514 *Quantitative Error Estimates*

515 From the trend calculations, error statistics showed around ± 0.1 kg S/ha /yr on average for the
516 SO_4^{2-} wet deposition trend for grid cells with relatively high trend magnitudes. The actual error
517 across the domain varied based on the magnitude of the NADP site distribution. Likewise, the
518 OMI SO_2 trend calculation carried a ± 0.001 to ± 0.0025 DU/yr uncertainty, with greater
519 uncertainties for grid boxes with low SO_2 amounts or low trends. Interpolation of irregular
520 spaced data such as the case of NADP sites (Figure 2a), inherently carries uncertainty due to
521 varying site coverage and the interpolation method itself. The uncertainty was in the 10-20%
522 error range for more than half the grid boxes in the domain, while areas with less observing sites
523 contained higher percent error. The error analysis was performed through validation of annual
524 wet deposition output from the Community Multi-scale Air Quality (CMAQ) model. These
525 interpolation errors, while having potential impacts on the results, could not be avoided due to
526 limitation of the NADP observing network.

527 The error in the percent contributions results directly from the uncertainties in the
528 normalized trends and the PSCF, as those are the two components used in the calculation (Eq. 3).

529 Uncertainties in the PSCF can originate from trajectory calculations and from different
530 possibilities of choosing the threshold. Changing the threshold by ± 1 ppb resulted in only 25-30
531 of the 2400 grid boxes in the domain having a PSCF change of greater than 0.1, as determined by
532 a sensitivity test. Therefore, the overall result across the domain is not significantly affected by
533 this parameter. The calculations of the trajectories inherently contained errors as a result of
534 limited temporal and spatial resolutions of the model reanalysis meteorological data. However,
535 given the spatial resolution of the OMI instrument, the resolution of the meteorological data was
536 appropriate. We can still estimate roughly 20% relative uncertainty, which is proportional to
537 trajectory distance (Stohl, 1998). In regards to the normalized trends, the grid cells with high
538 trends were estimated through sensitivity tests to have an uncertainty on the order of 20-30%,
539 accounting for OMI and NADP data uncertainty in addition to the normalized trend calculations.
540 In grid boxes with smaller trends, the uncertainty is higher because their weight is closer to 0.
541 However, the areas with low SO_2 and SO_4^{2-} trends generally do not strongly impact the results
542 presented. The total uncertainties in the percent contribution can be estimated to have an upper
543 limit 30-40% in most grid cells of the domain, as an upper limit. This result was obtained by
544 combining the square error of the PSCF and the two normalized trends.

545 *Other Limitations and Uncertainties*

546 One big limitation in this study is the characteristics of wet deposition. Whether the SO_4^{2-} is
547 being deposited or carried further downwind is dependent on nature of the trajectory and if
548 precipitation occurred. Given the uncertainties in diagnosing rain or cloud formation events
549 along the trajectory, we primarily focus on determining where deposition is highly decreasing
550 along with an active flow pattern from trajectory analysis showing possible origins of SO_4^{2-} from
551 nearby sulfur in the atmosphere. The trajectories are utilized as rough interpretations of air flow
552 and to contribute to a seasonal climatology as shown in Section 2. Furthermore, HYSPLIT model

553 parameters were rather simple in the sense that the model was not run at multiple times during
554 the day or from different heights. We kept the constant initialization height of 500 m (above
555 ground) which is a reasonable representation of mid boundary layer height. The back trajectories
556 were only run once a day to match the temporal resolution of OMI and around the time the
557 instrument would pass over the Eastern U.S to make measurements. Due to keeping the
558 initialization time constant at 18Z and the height at 500 meters, there could have been error
559 associated with analyzing the trajectories with respect to high SO₂ amounts since these can
560 change due to weather patterns and within hours. Another limitation was the difficulty in
561 distinguishing between sulfate coming from rainout or washout. With the nature of the data,
562 relative simplicity of HYSPLIT and lack of a chemistry model, there was not much information
563 that could be gathered regarding the exact origin of the sulfate. However, we would expect a lot
564 of the sulfur from power plants to be found closer to the surface than aloft, consistent with the
565 500m trajectory initial height. Overall, chemistry related factors such as how much of the SO₂ is
566 converted to SO₄²⁻ on a daily basis, how much is exported or removed through other pathways,
567 and cloud processes could not be adequately captured by the method, therefore producing
568 additional uncertainty in the results. Lastly, in many cases, the trajectories and the sulfur residing
569 in the atmosphere can be influenced by local and smaller scale meteorology, in addition to the
570 synoptic airflow. This can complicate the deposition and sulfur dioxide transport and can lead to
571 a loss of important information regarding the connection between the two trends. These
572 uncertainties are difficult to quantify but likely do not strongly impact the conclusions of the
573 study, because the lifetime of SO₂ is relatively short and wet deposition is a main sink.
574 Addressing complexities in the future, as opposed to this simplified approach, might gain
575 additional insight on the link between the two trends.

576 There is also possibility of biases in precipitation collection based on the collector
577 instrument used (Wetherbee et al, 2009). Likewise, the OMI retrieval of SO₂ while much
578 improved over the years, still has substantial noise and errors and could also have had a minor
579 effect on the calculated trends. Another source of error in the method itself could be the low
580 detection rates of SO₂ exceeding a threshold at a site. This happens during summer when the
581 exceedance rate was low compared to winter, resulting in a more scattered PSCF and
582 contribution maps. The resulting PSCF calculation (Eq. 1) would be fairly sporadic as m would
583 be low compared to the total number of trajectories (n). Since calculating percent contribution
584 was heavily based on PSCF (Eq. 3), some grid boxes may not be represented as accurately,
585 especially in JJA and at low SO₂ sites (Wilmington and Beltsville). It is important to note that
586 these methods are mostly probabilistic, meaning we cannot discern concrete locations and say
587 with complete certainty that a specific source contributed to the deposition changes.

588 **4. Summary and Conclusions**

589 In summary, the origin of pollutants in acidic wet deposition can be determined with a
590 combination of in situ and satellite observations coupled to trajectory analysis. In this study we
591 quantified the possible origin of SO₄²⁻ wet deposition for five sites in the eastern United States
592 over 2005-2015. Each site showed characteristic source regions, generally consistent with
593 seasonal wind patterns and observed SO₂ from OMI. Dominant sources depend on prevailing
594 westerly winds, faster summer rates of SO₂ oxidation, and the synoptic conditions associated
595 with precipitation. We also find that contribution changes pattern in direction and range with the
596 season.

597 Reported emissions, observed concentrations, and monitored deposition all tell a
598 consistent story – efficient scrubbing SO₂ in the eastern US has led to dramatic improvements in
599 SO₄²⁻ wet deposition in the same region and benefits are generally seen within 500 km of the

600 source. At the Beltsville, MD site in winter, about 2/3 of the SO_4^{2-} wet deposition originates
601 from the west and 1/3 from the east, in keeping with the dominance of westerly winds. In
602 summer, when SO_2 has a shorter lifetime with respect to oxidation to SO_4^{2-} , closer emitters
603 generally have a greater influence – the bulk of the deposition (80%) is due to sources < 300 km
604 away; in winter this range is expanded to over 500 km. Nearby sources to the east do however
605 have a substantive impact in colder months. The winter season is associated with a higher
606 frequency of strong mid-latitude extratropical weather systems, which will produce periods of
607 northeasterly winds off the Atlantic Ocean and larger amounts of moisture and precipitation.
608 Likewise, wind direction becomes more variable and, on average, weaker during the summer
609 months. The region also experiences less precipitation during the summer, with the exception of
610 heavy localized precipitation in convective storms. Nonetheless, 2/3 of the contribution (Table 4)
611 is from east of the site, indicating the importance of source proximity and summer weather
612 patterns. Both statewide emission controls and those upwind, out-of-state appear to have
613 contributed to the decreasing SO_4^{2-} deposition trend. While higher contribution values come from
614 several grid boxes within 100 km of the Beltsville site for the 2008-2012 period, the accumulated
615 contribution in the southwest PA region has arguably more effect on the full ten year deposition
616 trend overall. At the Hackney, OH site, the summer-winter difference is weaker, with 80% of the
617 deposition from within ~400 km in both seasons, reflecting sources located closer to the site.
618 Despite major SO_2 sources to the east, transport of sulfur from the west dominates, accounting
619 for 2/3 of the deposition in the summer, and 9/10 in the winter. At this site, the prevailing wind
620 pattern rather than proximity to emitters is the governing factor for this distribution.

621 Without the implementation of the appropriate methodology, such as the trajectory
622 analysis used in this work, the regional SO_2 concentrations and deposition could not be
623 adequately linked given their geographic displacement. The satellite data provide a consistent

624 context for interpreting in-situ measurements and trajectory-based PCSF analyses, allowing us to
625 identify major source areas that contribute to the observed decreases in SO_4^{2-} wet deposition.
626 Future work will incorporate further modeling in addition to the statistical method used in this
627 study. Additional meteorological analyses can also be useful in determining the role of seasonal
628 precipitation patterns and climatology on wet deposition rates. Lastly, a larger sample size of
629 sites and extension of the trajectory climatology to more years in the model and statistical
630 method may increase the robustness and accuracy of the results. Although other locations
631 worldwide are characteristically different from the eastern United States, the methods presented
632 here may prove useful in areas currently planning new emission and pollution reductions such as
633 East and South Asia, and could help guide the selection of key targets for pollution control.
634 Sources from the direction associated with precipitation during the season with greater oxidant
635 (OH and H_2O_2) concentrations may play an outsized role in acid precipitation. The method can
636 be particularly useful for in situ data-poor areas, given that satellite data will help to capture the
637 fast-paced changes in emissions and provide more frequent updates than conventional bottom-up
638 emission inventories.

639 **Acknowledgements:**

640 We would like to thank the NASA Earth Science Division (ESD) Aura Science Team program
641 for funding of the OMI SO_2 product development and analysis (Grant # 80NSSC17K0240). The
642 OMI project is managed by the Royal Meteorological Institute of the Netherlands (KNMI) and
643 the Netherlands Space Agency (NSO). We also acknowledge partial support for this study from
644 NASA's Earth Science New Investigator Program (Grant # NNX14AI02G). Additionally, we
645 thank Hao He for providing CMAQ model results for the error analysis of the interpolation
646 method and Jon Poterjoy for providing additional input for the text of this paper.

647

648 **References:**

- 649 Begum, B. A., Kim, E., Jeong, C.-H., Lee, D.-W., & Hopke, P. K., (2005): Evaluation of the
650 potential source contribution function using the 2002 Quebec forest fire episode.
651 *Atmospheric Environment*, 39(20), 3719–3724. doi: 10.1016/j.atmosenv.2005.03.008
- 652 Brook, J.R, Samson P.J, Sillman, S. (1994): A meteorology-based approach to detecting the
653 relationship between changes in SO₂ emission rates and precipitation concentrations of
654 sulfate. *Journal of Applied Meteorology*, 33, pp. 1050-1066. doi: 10.1175/1520-
655 0450(1994)033<1050:AMBATD>2.0.CO;2
- 656 Butler, T.J, Likens, G.E, Stunder, B.J (2001). Regional-scale impacts of Phase I of the Clean Air
657 Act Amendments in the USA: The relation between emissions and concentrations, both
658 wet and dry. *Atmospheric Environment*. 35(6). 1015–1028. doi: 10.1016/S1352-
659 2310(00)00386-1
- 660 Charles T. Driscoll, Gregory B. Lawrence, Arthur J. Bulger, Thomas J. Butler, Christopher S.
661 Cronan, Christopher Eagar, Kathleen F. Lambert, Gene E. Likens, John L. Stoddard,
662 Kathleen C. Weathers; *Acidic Deposition in the Northeastern United States: Sources and*
663 *Inputs, Ecosystem Effects, and Management Strategies: The effects of acidic deposition*
664 *in the northeastern United States include the acidification of soil and water, which*
665 *stresses terrestrial and aquatic biota*, *BioScience*, Volume 51, Issue 3, 1 March 2001, pp
666 180–198. doi: 10.1641/0006-3568(2001)051[0180:ADITNU]2.0.CO;2
- 667 Chen, L. W. A., Doddridge, B. G., Dickerson, R. R., Chow, J. C., & Henry, R. C. (2002). Origins
668 of fine aerosol mass in the Baltimore–Washington corridor: Implications from
669 observation, factor analysis, and ensemble air parcel back trajectories. *Atmospheric*
670 *Environment*, 36, 4541–4554. doi: 10.1016/S1352-2310(02)00399-0

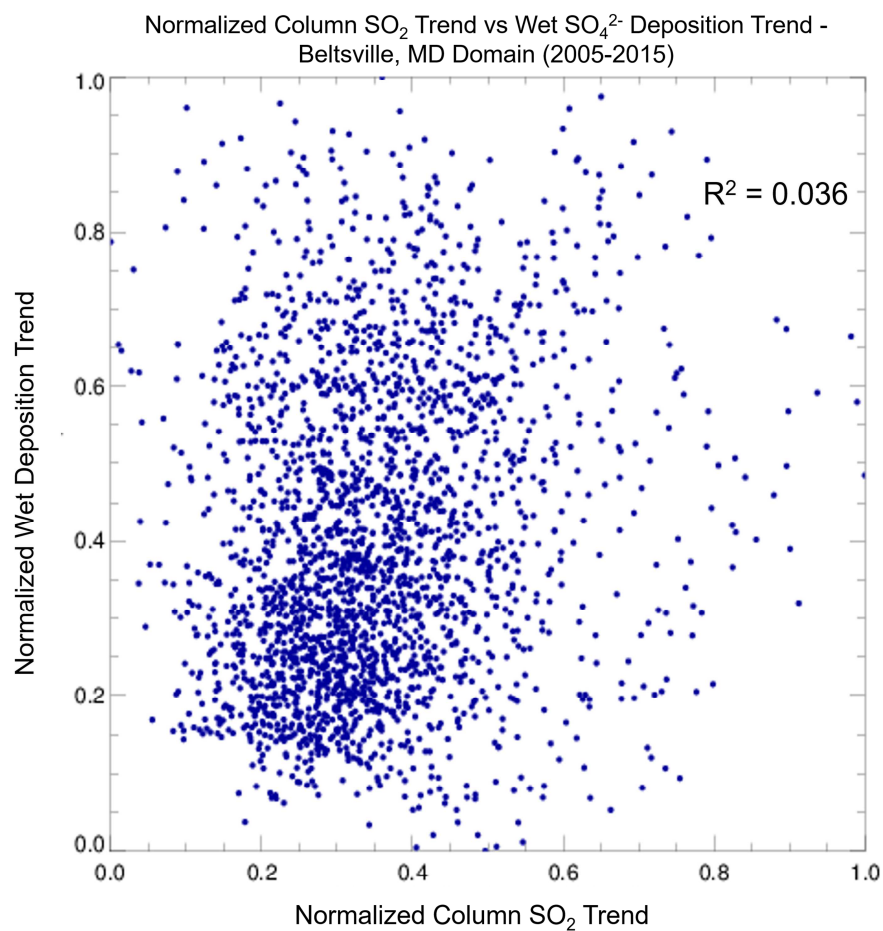
- 671 Driscoll, C.T., Driscoll, K.M., Roy, K.M., Mitchell, M.J., 2003. Chemical response of lakes in
672 the Adirondack region of New York to declines in acid deposition. *Environmental*
673 *Science and Technology* 37 (10), pp 2036-2042. doi: 10.1021/es020924h
- 674 Dutkiewicz, V. A.; Das, M.; Husain, L. The relationship between regional SO₂ emissions and
675 downwind aerosol sulfate concentrations in the northeastern U.S., *Atmos. Environ.* 2000,
676 34, 1821- 1832. doi: 10.1016/S1352-2310(99)00334-9
- 677 Fioletov, V. E., C. A. McLinden, N. Krotkov, M. D. Moran, and K. Yang (2011): Estimation of
678 SO₂ emissions using OMI retrievals, *Geophys. Res. Lett.*, **38**, L21811, doi:
679 10.1029/2011GL049402.
- 680 Fioletov, V. E., McLinden, C. A., Krotkov, N., and Li, C.: Lifetimes and emissions of SO₂ from
681 point sources estimated from OMI, *Geophys. Res. Lett.*, 42, 1969–1976,
682 doi:10.1002/2015GL063148, 2015
- 683 Gao, N., Cheng, M.D., Hopke, P.K., 1993. Potential source contribution function analysis and
684 source apportionment of sulfur species measured at Rubidoux, CA during the southern
685 California air quality study, 1987. *Analytica Chimica Acta* 277, 369–380. doi:
686 10.1016/0003-2670(93)80449-U
- 687 Geddes, J. A. and Martin, R. V.: Global deposition of total reactive nitrogen oxides from 1996 to
688 2014 constrained with satellite observations of NO₂ columns, *Atmos. Chem. Phys.*, 17,
689 10071–10091, 2017, <https://doi.org/10.5194/acp-17-10071-2017>
- 690 He, H., Vinnikov, K., Li, C., Krotkov, N. A., Jongeward, A. R., Li, Z., Stehr, J. W., Hains, J. C.,
691 and Dickerson, R. R (2016).: Response of SO₂ and particulate air pollution to local and
692 regional emission controls: A case study in Maryland, *Earth's Future*,
693 doi:10.1002/2015EF000330

- 694 Heo, J., McGinnis, J.E., de Foy, B., Schauer, J.J., (2013): Identification of potential source areas
695 for elevated PM_{2.5}, nitrate and sulfate concentrations. *Atmos. Environ.* 71, 187–197. doi:
696 10.1016/j.atmosenv.2013.02.008
- 697 Krotkov, N., McLinden, C.A, Li, C., L.N. Lamsal, Celarier, E. A., Marchenko, S. V., Swartz, W.
698 H., Bucsela, E., Joiner, J., Duncan, B, Boersma, F., Veeffkind, P., Levelt, P., Fioletov, V.,
699 Dickerson, R. R., He, H., Lu, Z., and Streets, D., 2016: Aura OMI observations of
700 regional SO₂ and NO₂ pollution changes from 2005-2015. *Atmos. Chem. Phys.*, 16,
701 4605–4629. doi: 10.5194/acp-16-4605-2016
- 702 Lamb, D., and V. Bowersox. 2000. The national atmospheric deposition program: an overview.
703 *Atmos Environ.* 34:1661–1663. doi: 10.1016/S1352-2310(99)00425-2
- 704 Lee, C., et al. (2011), SO₂ emissions and lifetimes: Estimates from inverse modeling using in situ
705 and global, space-based (SCIAMACHY and OMI) observations, *J. Geophys. Res.*, 116,
706 D06305. doi: 10.1029/2010JD014758
- 707 Likens, G. E., Driscoll, C.T., Buso, D.C., Mitchell, M. J., Lovett, G. M., Bailey, S. W., Siccama,
708 T. G., Reiners, W. A., Alewell, C. (2002), The biogeochemistry of sulfur at Hubbard
709 Brook, *Biogeochemistry*, 60(3), 235-316.
- 710 McLinden, C. A., Fioletov, V., Shephard, M. W., Krotkov, N., Li, C., Martin, R. V., et al. 2016:
711 Space-based detection of missing sulfur dioxide sources of global air pollution. *Nature*
712 *Geoscience*, 9(7), 496–500. doi: 10.1038/ngeo2724
- 713 National Atmospheric Deposition Program, 2016. Total Deposition 2015 Annual Map Summary.
714 NADP Data Report 2016-02. Illinois State Water Survey, University of Illinois at
715 Urbana-Champaign, IL.

- 716 NASA Goddard Earth Sciences: Aura OMI Sulphur Dioxide Data Product-OMSO2, available at:
717 http://disc.sci.gsfc.nasa.gov/Aura/data-holdings/OMI/omso2_v003.shtml, Accessed
718 2017.
- 719 Pekney, Natalie J., Davidson, Cliff I., Zhou, Liming, Hopke, Philip K. (2006): Application of
720 PSCF and CPF to PMF-Modeled Sources of PM_{2.5} in Pittsburgh, *Aerosol Science and*
721 *Technology*, 40:10, 952-961. doi: 10.1080/02786820500543324
- 722 Polissar, A. V., Hopke, P.K., Paatero, P., Kaufmann, Y.J., Hall, D.K., Bodhaine,
723 B.A., Dutton, E.G., Harris, J.M. (1999). The aerosol at Barrow, Alaska: Long-term
724 trends and source locations, *Atmos Environ.*, 33, pp. 2441-2458. doi: 10.1016/S1352-
725 2310(98)00423-3
- 726 Samson, P. J., 1981: Trajectory Analysis of Summertime Sulfate Concentrations in the Northeast
727 United States. *Journal of Applied Meteorology*, 19, 1382–1394. doi: 10.1175/1520-
728 0450(1980)019<1382:TAOSSC>2.0.CO;2
- 729 Shah, V., Jaeglé, L., Thornton, J. A., Lopez-Hilfiker, F. D., Lee, B. H., Schroder, J. C.,
730 Campuzano-Jost, P., Jimenez, J. L., Guo, H., Sullivan, A. P., Weber, R. J., Green, J. R.,
731 Fiddler, M. N., Bililign, S., Campos, T. L., Stell, M., Weinheimer, A. J., Montzka, D. D.,
732 and Brown, S. S. (2018): Chemical feedbacks weaken the wintertime response of
733 particulate sulfate and nitrate to emissions reductions over the eastern United States, P.
734 *Natl. Acad. Sci. USA*, <https://doi.org/10.1073/pnas.1803295115>
- 735 Shannon, J.D. (1997) Scales of sulfur concentrations and deposition from the perspective of
736 the receptor. *Atmos. Environ.* 31, 3933–3939. doi:10.1016/S1352-2310(97)00242-2

- 737 Shannon, J.D. Regional Trends in Wet Deposition of Sulfate in the United States and
738 SO₂ Emissions from 1980 through 1995; *Atmos. Environ.* 1999, 33 (5), 807-816. doi:
739 10.1016/S1352-2310(98)00143-5
- 740 Stein, A.F., Draxler, R.R, Rolph, G.D., Stunder, B.J.B., Cohen, M.D., and Ngan, F., (2015).
741 NOAA's HYSPLIT atmospheric transport and dispersion modeling system, *Bull. Amer.*
742 *Meteor. Soc.*, **96**, 2059-2077. doi: 10.1175/BAMS-D-14-00110.1
- 743 Stohl, A.: Computation, accuracy and applications of trajectories – a review and bibliography,
744 *Atmos. Environ.*, 32, 947–966, 1998. [https://doi.org/10.1016/S1352-2310\(97\)00457-3](https://doi.org/10.1016/S1352-2310(97)00457-3)
- 745 U.S. EPA (United States Environmental Protection Agency). 2017. Data from the Clean Air
746 Status and Trends Network. Accessed 2017. <https://www.epa.gov/castnet>
- 747 U.S. EPA. (2002): EPA Acid Rain Program 2001 Progress Report. EPA-430-R-02-009. Clean
748 Air Markets Program, Office of Air and Radiation, Nov 2002.
- 749 U.S. EPA. (2003):. Latest findings on national air quality: 2002 status and trends. EPA/454/K-
750 03/001. Research Triangle Park, NC.
- 751 U.S. EPA. (2015): The Clean Air Act – Highlights of the 1990 Amendment.
752 [https://www.epa.gov/sites/production/files/2015-11/documents/the_clean_air_act_-](https://www.epa.gov/sites/production/files/2015-11/documents/the_clean_air_act_-_highlights_of_the_1990_amendments.pdf)
753 [_highlights_of_the_1990_amendments.pdf](https://www.epa.gov/sites/production/files/2015-11/documents/the_clean_air_act_-_highlights_of_the_1990_amendments.pdf)
- 754 Vet, R., Artz, R. S., Carou, S., Shaw, M., Ro, C.-U., Aas, W., Baker, A., Bowersox, V. C.,
755 Dentener, F., Galay-Lacaux, C., Hou, A., Pienaar, J. J., Gillet, R., Forti, M. C., Gromov,
756 S., Hara, H., Khodzher, T., Mahowald, M., Nickovic, S., Rao, P. S. P., and Reid, N. W.
757 (2014): A global assessment of precipitation chemistry and deposition of sulfur, nitrogen,
758 sea salt, base cations, organic acids, acidity and pH, and phosphorus, *Atmos. Environ.*,
759 93, 3– 100, doi:10.1016/j.atmosenv.2013.10.060

- 760 Wang, Y., Zhang, X., & Draxler, R. R. TrajStat, 2009: GIS-based software that uses various
761 trajectory statistical analysis methods to identify potential sources from long-term air
762 pollution measurement data. *Environmental Modelling & Software*, 24(8), 938–939.
763 doi:10.1016/j.envsoft.2009.01.004
- 764 Wetherbee, G. A., 2017: Precipitation collector bias and its effects on temporal trends and spatial
765 variability in National Atmospheric Deposition Program/National Trends Network data.
766 *Environmental Pollution*, 223, 90–101. doi:10.1016/j.envpol.2016.12.036
- 767 Zhang, Z. Y., M. S. Wong, and K. H. Lee (2015), Estimation of potential source regions of
768 PM_{2.5} in Beijing using backward trajectories, *Atmos. Pollut. Res.*, 6(1), 173–177.
769 doi:10.5094/APR.2015.020.
- 770 Qu L.L, Xiao H.Y, Zheng N.J, Zhang Z.Y, Xu Y. Comparison of four methods for spatial
771 interpolation of estimated atmospheric nitrogen deposition in South China. *Environ Sci*
772 *Pollut Res.* 2016. doi: 10.1007/s11356-016-7995-0

773 **Appendix A:**

774

775 Figure A.1: A scatter plot of the normalized trends for the Beltsville, MD site domain. Each
776 point represents a grid box in the domain with a unique normalized SO₂ and SO₄²⁻ wet deposition
777 trend value. The bounds for the domain are [88.875°, 73.875° W] and [35.125°, 45.125° N].

778

779

780

781

Table A.1: Cumulative distribution of winter (DJF) percent contribution to SO_4^{2-} deposition trend at the Beltsville, MD site within given ranges from the site. The totals are summed through each distance range and are broken up by direction with respect to the longitude of the site. The first column is the distance range from the site over which the contribution of grid boxes is summed. The last column is the percent contribution for only the single distance range, not the cumulative amount.

Distance from Site (km)	East	West	Total	Incremental difference (between two radii)
0-50	3.11	0.24	3.35	3.35
50-100	17.04	1.74	18.78	15.43
100-200	33.1	11.34	44.44	25.66
200-300	34.31	21.67	55.98	11.54
300-400	35.51	35.54	71.05	15.07
400-500	35.62	41.88	77.5	6.45
500-1000	35.62	62.41	98.03	20.53

782

Table A.2: Same as Table A.1 but for summer (JJA)

Distance from Site (km)	East	West	Total	Incremental difference (between two radii)
0-50	0.00	0.00	0.00	0.00
50-100	0.81	2.09	2.90	2.90
100-200	27.86	14.11	41.97	39.07
200-300	63.05	19.47	82.52	40.55
300-400	66.36	19.47	85.83	3.31
400-500	65.34	21.02	86.36	0.53
500-1000	66.37	32.87	99.24	12.88

783

784

Table A.3: Cumulative distribution of winter (DJF) percent contribution to SO_4^{2-} wet deposition trend at the Hackney, OH site within given ranges from the site. The totals are summed through each distance range and are broken up by direction with respect to the longitude of the site. The first column is the distance range from the site over which the contribution of grid boxes is

summed. The last column is the percent contribution for only the single distance range, not the cumulative amount.

Distance from Site (km)	East	West	Total	Incremental difference (between two radii)
0-50	4.93	5.94	10.87	8.71
50-100	6.91	16	22.91	12.04
100-200	9.01	38.16	47.17	24.26
200-300	9.09	53.96	63.05	15.88
300-400	9.09	67.9	76.99	13.94
400-500	9.28	76.62	85.9	8.91
500-1000	9.28	90.72	100	14.1

785

Table A.4: Same as Table A.3 but for summer (JJA)

Distance from Site (km)	East (%)	West (%)	Total (%)	Incremental difference (between two radii)
0-50	2.95	1.75	4.70	4.703
50-100	5.56	5.438	11.00	6.297
100-200	18.14	20.67	38.81	27.81
200-300	29.10	37.01	66.11	27.3
300-400	31.16	47.06	78.22	12.11
400-500	31.70	54.73	86.43	8.205
500-1000	31.87	67.15	99.02	12.595

786

Highlights:

- Sulfate deposition trends attributed to reduction of emissions from specific areas.
- Trajectory and contribution analysis used to find potential source regions
- Reductions in large SO₂ sources dominate deposition trends near Ohio River Valley
- Key differences between winter and summer contribution to deposition
- Deposition in Maryland decreased due to emission control both in and out of state.